

# The Solvophobic Solvation and Interaction of Small Apolar Particles in Imidazolium-Based Ionic Liquids is Characterized by Enthalpy-/Entropy-Compensation

Dietmar Paschek,<sup>1,\*</sup> Thorsten Köddermann,<sup>2</sup> and Ralf Ludwig<sup>2,3</sup>

<sup>1</sup>*Physikalische Chemie, Fakultät Chemie, TU Dortmund,  
Otto-Hahn-Str. 6, D-44221 Dortmund, Germany*

<sup>2</sup>*Physikalische und Theoretische Chemie, Institut für Chemie,  
Universität Rostock, Dr.-Lorenz-Weg 1, D-18059 Rostock, Germany*

<sup>3</sup>*Leibniz Institut für Katalyse an der Universität Rostock,  
Albert-Einstein-Str. 29a, D-18059 Rostock, Germany*

(Dated: November 19, 2018)

We report results of molecular dynamics simulations characterizing the solvation and interaction of small apolar particles such as methane and Xenon in imidazolium-based ionic liquids (ILs). The simulations are able to reproduce semi-quantitatively the anomalous temperature dependence of the solubility of apolar particles in the infinite dilution regime. We observe that the “solvophobic solvation” of small apolar particles in ILs is governed by compensating entropic and enthalpic contributions, very much like the hydrophobic hydration of small apolar particles in liquid water. In addition, our simulations clearly indicate that the solvent mediated interaction of apolar particles dissolved in ILs is similarly driven by compensating enthalpic/entropic contributions, making the “solvophobic interaction” thermodynamically analogous to the hydrophobic interaction.

Ionic liquids (ILs) are a new class of solvents for use in environmentally benign industrial processes and are seen as alternative to toxic volatile organic compounds [1, 2, 3]. The ionic nature of ILs has important consequences for the structure of the liquid on the nanoscopic level [4, 5]. Spectroscopic evidence is suggesting the presence and importance of the formation of intermolecular cation/anion hydrogen bonds [6]. Favorable and specific ion/cation interactions seem to induce the formation of a persistent anion/cation network, which has been shown to be quite tolerable to adding both polar and apolar particles [7]. Quite recently, systematic measurements of the infinite dilution properties for a number of gases, including methane, carbon dioxide, as well as the noble gases have been reported [8, 9, 10, 11]. The experimental data indicate that imidazolium-based ILs of type 1-alkyl-3-methylimidazolium bis(trifluoromethylsulfonyl)imide (denoted as  $[C_n\text{mim}][\text{NTf}_2]$ ) exhibit an anomalous temperature dependence of the solubility of apolar compounds showing a decreasing solubility with increasing temperature [10]. Moreover, it was observed that the anomalous behavior is found to be even strengthened with increasing particle size. We have recently developed an improved (nonpolarizable) all-atom forcefield for imidazolium based ILs of the type  $[C_n\text{mim}][\text{NTf}_2]$  and have shown that a number of thermodynamical and dynamical properties of the pure IL could be reproduced almost quantitatively [12]. Here we show that our forcefield is also capable of semi-quantitatively describing the solvation behavior of small apolar particles. More importantly, we clearly demonstrate that the solvation is characterized by an enthalpy-/entropy-compensation-effect, qualitatively similar to the behavior of the hydrophobic hydration of

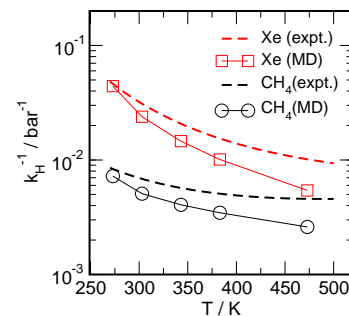


FIG. 1: Solubility (here given as inverse Henry’s constant for the case of infinite dilution with  $k_H^{-1} = \exp[\beta \mu_{ex, Gas}^l] / \rho_{IL}^l RT$  [17]) of Methane and Xenon in  $[C_6\text{mim}][\text{NTf}_2]$  at atmospheric pressure conditions. The symbols indicate data obtained from MD simulations using our IL-forcefield [12] determined from the potential distribution theorem [18]. The experimental data is according to Maurer et al. [10].

small apolar particles in liquid water [13, 14, 15, 16]. In addition, we determine for the first time the existence of a “solvophobic interaction” of apolar particles in ILs which is stabilized by entropic and counter-balanced by enthalpic contributions, similar to the hydrophobic interaction of small solutes in water.

We perform constant pressure (NPT) MD simulations of imidazolium based ILs of the type  $[C_2\text{mim}][\text{NTf}_2]$  and  $[C_6\text{mim}][\text{NTf}_2]$  at a pressure of 1 bar over the temperature range of 273 K up to 907 K [22] of system-sizes of 173 ion pairs using our IL forcefield [12]. Simulations of at least 10 ns length are employed for each state-point. The simulation conditions [23] are similar as in Ref. [12]. All simulations are performed with the Gromacs 3.2 simulation program [24]. We study the solvation of small apolar

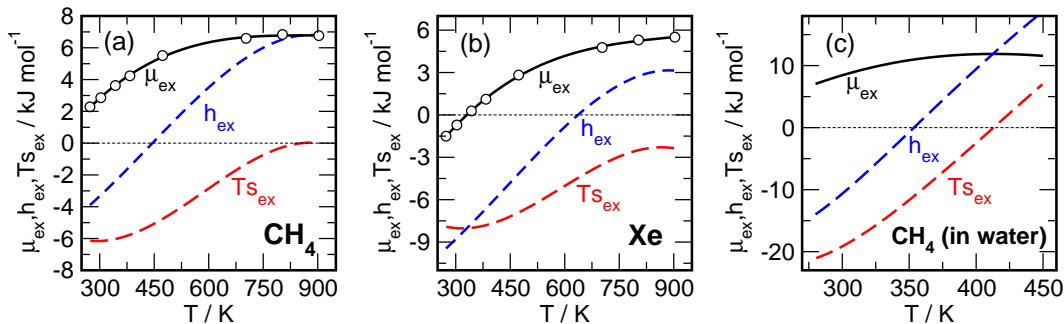


FIG. 2: Simulated excess chemical potential  $\mu_{ex}$ , as well as its enthalpic and entropic contributions  $\mu_{ex} = h_{ex} - Ts_{ex}$  of (a) Methane and (b) Xenon in  $[\text{C}_2\text{mim}][\text{NTf}_2]$ , as well as (c) Methane in water (all at atmospheric pressure conditions). The symbols represent the data obtained from the simulations applying the potential distribution theorem [18]. Enthalpic and entropic contributions in a,b were derived from fitting the  $\mu_{ex}(T)$ -data to a third order polynome (shown as black solid line [19]). The experimental data for the solvation of Methane in water shown in (c) are according to Refs. [20, 21].

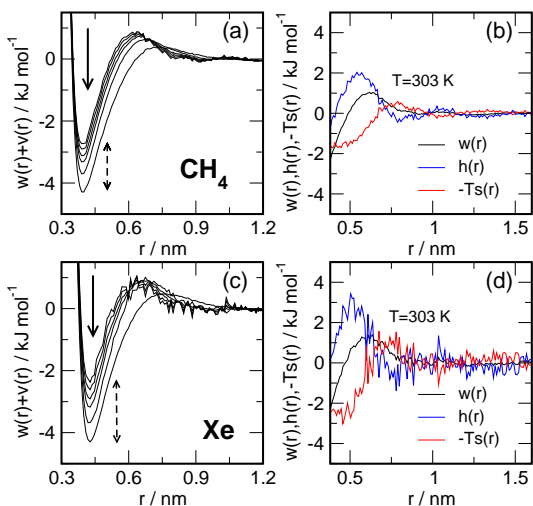


FIG. 3: a,c) profile of free energy  $\Delta\mu_{ex}(r) = w(r) + v(r)$  for the association of two Methane (a) and Xenon (c) particles with increasing temperature. Here  $v(r)$  is the intermolecular potential, whereas  $w(r)$  denotes the solvent contribution to the free energy profile. The shown temperatures are 273 K, 303 K, 343 K, 383 K, 473 K, and 703 K. The arrow indicates increasing temperature. b,d) solvent contribution to the profile of the free energy, as well as the enthalpic and entropic contributions obtained for  $T = 303$  K. Methane (b). Xenon (d).

particles for the for the case of Methane and Xenon represented by single Lennard-Jones spheres with parameters ( $\sigma_{\text{Me-Me}} = 0.3730$  nm,  $\epsilon_{\text{Me-Me}}/k = 147.5$  K, and  $\sigma_{\text{Xe-Xe}} = 0.3975$  nm,  $\epsilon_{\text{Xe-Xe}}/k = 214.7$  K) [25] applying Lorentz-Berthelot mixing rules [26] for all cross-terms. The solvation free energy per particle is given by the excess chemical potential  $\mu_{ex}$ . We determined  $\mu_{ex}$  for the case of infinite dilution a posteriori from the IL MD-trajectories applying Widom’s potential distribution theorem [18] with  $\mu_{ex} = -kT \ln \langle V \exp(-\beta \Phi(\vec{r})) \rangle / \langle V \rangle$ . Here is  $\beta = 1/kT$ ,  $V$  the volume of the simulation box,

and  $\Phi(\vec{r})$  is the energy of a randomly inserted (gas) test-particle at position  $\vec{r}$ . The brackets  $\langle \dots \rangle$  indicate isobaric isothermal sampling as well as sampling over many different positions  $\vec{r}$ . More details about the calculation are available in Ref. [25]. The solubility of the gas-particles is given as the inverse Henry’s constant  $k_H^{-1} = \exp[\beta \mu_{ex,\text{Gas}}^l / \rho_{\text{IL}}^l RT]$  [17] where  $\mu_{ex,\text{Gas}}^l$  is the chemical potential of the solute in the liquid phase and  $\rho_{\text{IL}}^l$  is the average number density of the ionic liquid. Note that the number density of neutral ion-pairs is used here.

Figure 1 compares the solubility of Methane and Xenon in  $[\text{C}_6\text{mim}][\text{NTf}_2]$  as obtained from our MD simulations with solubility data recently published by Maurer et al. [10]. We would like to emphasize that without any refinement of the potential parameters, the solubility-data is quite satisfactorily reproduced. For low temperatures the agreement is almost quantitatively. In addition, the particle-size dependence is well described. We would particularly like to stress the fact that both simulation and experiment indicate an *anomalous* temperature dependence, showing a decreasing solubility with increasing temperature, very much resembling the solvation of apolar gases in water [27]. It is the purpose of this letter to demonstrate that the analogy to the “hydrophobic effect” is much more deep-rooted thermodynamically.

In Figure 2 we show the excess chemical potentials of Methane and Xenon dissolved in  $[\text{C}_2\text{mim}][\text{NTf}_2]$ . For comparison the excess chemical potential of Methane in liquid water is given. The increasing chemical potential with increasing temperature equivalent to the anomalous solvation. In analogy to the procedure used in Ref. [25] the data points shown in Figure 2 were fitted to a third order polynome [19] and the corresponding entropic and enthalpic contributions were determined from the temperature dependence of the fitted  $\mu_{ex}(T)$  with  $s_{ex} = -(\partial\mu_{ex}/\partial T)_{T,P}$  and  $h_{ex} = \mu_{ex} + Ts_{ex}$ . From Figure 2a,b it is evident that for the low temperature regime the negative heat of solvation  $h_{ex}$  is counter com-

compensated by a negative solvation entropy  $s_{ex}$ . Moreover, the heat of solvation exhibits a positive slope, revealing a positive solvation heat capacity contribution of about  $22 \text{ JK}^{-1}\text{mol}^{-1}$  for Methane and about  $26 \text{ JK}^{-1}\text{mol}^{-1}$  for the temperature interval between 300 K and 400 K. Both, the entropy/enthalpy compensation effect, as well as the positive heat capacity are also qualitative signatures of the hydrophobic hydration of small apolar particles in water [14, 28]. However, the solvation heat capacity is about a factor of five to six smaller, and the corresponding solvation entropies are about a factor of three to four smaller compared to the solvation in water (compare with Figure 2c and data in Ref. [25]). In addition, the maximum of  $\mu_{ex}(T)$ , which is observed in water around 410 K to 420 K is shifted to about 900 K to 1000 K for the case of  $[\text{C}_2\text{mim}][\text{NTf}_2]$ . The latter values are of course hypothetical, since the real ILs are not chemically stable under those extreme conditions. Our simulations indicate the anomalous solvation behavior of ILs is simply stretched out on a much broader temperature scale compared to water.

In addition to the solvation behavior, we also determine the solvent mediated interaction between two (identical) gas particles. Therefore we calculate the profile of free energy for the association process by applying the potential distribution theorem [18] with  $w(r) = -kT \ln \langle V \exp(-\beta \Phi(\vec{r}_1, \vec{r}_2)) \delta(|\vec{r}_1 - \vec{r}_2| - r) \rangle / \langle V \rangle - 2\mu_{ex}$ . Here  $\Phi(\vec{r}_1, \vec{r}_2)$  is the energy of randomly inserting two gas particles.  $\mu_{ex}$  is the excess chemical potential of the individual gas particles. The solvent mediated interaction  $w(r)$  is related to the gas-gas pair distribution function  $g(r)$  according to  $-kT \ln g(r) = w(r) + v(r)$ , where  $v(r)$  is the intermolecular pair potential between the two gas particles.  $w(r)$  is also sometimes referred to a “cavity potential” [29]. Similar to the excess chemical potential,  $w(r)$  was calculated a posteriori from stored trajectory data using a Monte Carlo procedure. The calculated profiles of free energy, as well as the corresponding enthalpic and entropic contributions for the association of two Methane and Xenon particles are shown in Figure 3. The minimum of the profile of free energy shown in Figure 3a,c represents the state where two particles are in close contact. Differing from the the profile of free energy for small hydrophobic particles dissolved in water, there is no pronounced second minimum existing here. Hence, the presence of a clearly defined solvent separated state is missing, which is likely to be related to the much larger size of solvent molecules involved here compared to water. However, in parallel to the behavior in water, we do observe a deepening of the first minimum with increasing temperature. When comparing the well depth of the minima in Figure 3a,c, Xenon exhibits stronger temperature effect than Methane. To determine enthalpic and entropic contributions, we have fitted each  $r$ -histogram-point of the set of  $w(r, T)$ -histograms to a third order polynome with respect to  $T$ . The corresponding profiles

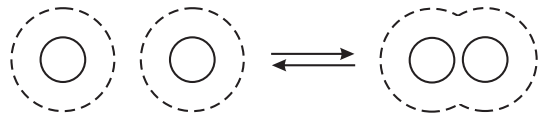


FIG. 4: Schematic diagram of the “solvophobic association” process. The contact configuration is stabilized with increasing temperatures by minimizing the entropy penalty.

calculated for  $T = 303 \text{ K}$  are shown in Figure 3b,d. The contact-state for both, Methane and Xenon is stabilized by the entropy part, whereas the enthalpic part mostly destabilizing. A simple explanation is based on the assumption that solvation enthalpy/entropy is mostly due to changes of the solvent in the first solvation shell, which is represented by the solvent accessible surface (SAS). In the contact state the SAS is minimized, leading to negative net entropy and positive net enthalpy for the association of two particles as depicted in Figure 4. Hence the association of apolar particles in ILs is driven by the tendency to *minimize the solvation entropy-penalty* (the phrase has been borrowed from Haymet et al. [30]) similar to what has been found for water [14, 30]. Consequently, the larger temperature dependence of the well depth of the profile of free energy observed for Xenon in Figure 3a,c is simply a consequence of its larger solvation entropy (compare data in Figures 2a,b).

Our simulations reveal interesting new insights into the solvation and interaction of apolar particles in ionic liquids. However, many questions remain unanswered. First of all, we have not shown what is exactly causing the entropy penalty of the “solovophobic solvation” in ILs. It might well be that the effect is similar to the hydrophobic hydration in water, where the entropy penalty has been largely attributed to the orientational bias put on the water molecules while trying to keep the hydrogen bond network around an apolar particle mostly intact [14]. Since the formation of intermolecular hydrogen-bonds is also an important feature in ILs [6], a similar mechanism might also apply here. However, it might also well be that the tendency to maximize anion-cation contacts in ILs [5] is introducing an ordering constraint in the solvation shell of an apolar particle and thus causing the entropy penalty. In addition, for the case of water it has been recognized recently that the solvation of small apolar particles, which is “entropy dominated”, is different than for large scale particles, which is “enthalpy dominated”. Hence there has to be a crossover, which has been placed on the  $< 1 \text{ nm}$ -scale as proposed by the theory of Lum et al. [16, 31]. The predicted size of the crossover-lengthscales were confirmed recently by computer simulations of Rajamani et al. [32] and by simulation based scaled-particle theory [33, 34]. Given the larger size of the IL molecules and considering the importance of maintaining anion/cation contacts, the crossover-lengthscale might be shifted to larger values for the case of ILs. Con-

sidering that the anomalous solvation behavior of gases increases with solute molecule-size [10, 11], the poor solubility of proteins in most pure ILs [35] might be a consequence of a pronounced solvation-entropy effect.

**Acknowledgments.** DP acknowledges gratefully support from the Deutsche Forschungsgemeinschaft (DFG SPP 1155) and from TU Dortmund. RL acknowledges financing by the state of Mecklenburg-Vorpommern, and partial support by the Deutsche Forschungsgemeinschaft.

---

\* Electronic address: dietmar.paschek@tu-dortmund.de

- [1] P. Wasserscheid and T. Welton, eds., *Ionic Liquids in Synthesis* (VCH-Wiley, Weinheim, 2008), 2nd ed.
- [2] R. D. Rogers and K. R. Seddon, *Science* **302**, 792 (2003).
- [3] F. Endres and S. Z. El Abedin, *Phys. Chem. Chem. Phys.* **8**, 2101 (2006).
- [4] J. N. A. C. Lopes and A. A. H. Padua, *J. Phys. Chem. B* **110**, 3330 (2006).
- [5] A. A. H. Padua, M. F. Gomes, and J. N. A. C. Lopes, *Acc. Chem. Res.* **40**, 1087 (2007).
- [6] T. Köddermann, C. Wertz, A. Heintz, and R. Ludwig, *ChemPhysChem* **7**, 1944 (2006).
- [7] L. P. N. Rebelo, J. N. C. Lopes, J. M. S. S. Esperanca, H. J. R. G. J. Lachwa, V. Najdanovic-Visak, and Z. P. Visak, *Acc. Chem. Res.* **40**, 1114 (2007).
- [8] J. L. Anthony, E. J. Maginn, and J. F. Brennecke, *J. Phys. Chem. B* **106**, 7315 (2002).
- [9] A. P. S. Kamps, D. Tuma, J. Z. Xia, and G. Maurer, *J. Chem. Eng. Data* **48**, 746 (2003).
- [10] J. Kumelan, A. P. S. Kamps, D. Tuma, and G. Maurer, *Ind. Eng. Chem. Res.* **46**, 8236 (2007).
- [11] J. L. Anthony, J. L. Anderson, E. J. Maginn, and J. F. Brennecke, *J. Phys. Chem. B* **109**, 6366 (2005).
- [12] T. Köddermann, R. Ludwig, and D. Paschek, *ChemPhysChem* **8**, 2464 (2007).
- [13] L. R. Pratt, *Annu. Rev. Phys. Chem.* **53**, 409 (2003).
- [14] N. T. Southall, K. A. Dill, and A. D. J. Haymet, *J. Phys. Chem. B* **106**, 521 (2002).
- [15] B. Widom, P. Bhimalapuram, and K. Koga, *Phys. Chem. Chem. Phys.* **5**, 3085 (2003).
- [16] D. Chandler, *Nature (London)* **437**, 640 (2005).
- [17] R. P. Kennan and G. L. Pollack, *J. Chem. Phys.* **93**, 2724 (1990).
- [18] B. Widom, *J. Chem. Phys.* **39**, 2808 (1963).
- [19] Fitted excess chemical potential  $\mu_{ex}(T) = \mu_0 + \mu_1 T + \mu_2 T^2 + \mu_3 T^3$  of Methane and Xenon in [C<sub>2</sub>mim][NTf<sub>2</sub>]. Methane:  $\mu_0 = -7.08 \times 10^0 \text{kJmol}^{-1}$ ,  $\mu_1 = 4.73 \times 10^{-2} \text{kJmol}^{-1} \text{K}^{-1}$ ,  $\mu_2 = -5.38 \times 10^{-5} \text{kJmol}^{-1} \text{K}^{-2}$ ,  $\mu_3 = 2.04 \times 10^{-8} \text{kJmol}^{-1} \text{K}^{-3}$ . Xenon:  $\mu_0 = -1.31 \times 10^1 \text{kJmol}^{-1}$ ,  $\mu_1 = 5.76 \times 10^{-2} \text{kJmol}^{-1} \text{K}^{-1}$ ,  $\mu_2 = -6.20 \times 10^{-5} \text{kJmol}^{-1} \text{K}^{-2}$ ,  $\mu_3 = 2.33 \times 10^{-8} \text{kJmol}^{-1} \text{K}^{-3}$ .
- [20] R. Fernandez-Prini and R. Crovetto, *J. Phys. Chem. Ref. Data* **18**, 1231 (1998).
- [21] W. Wagner and A. Pruß, *J. Phys. Chem. Ref. Data* **31**, 387 (2002).
- [22] [C<sub>2</sub>mim][NTf<sub>2</sub>]: Temperatures of 273.0 K, 303.0 K, 343.0 K, 383.0 K, 473.0 K, 703.3 K, 803.0 K, 903.0 K at a pressure of 1 bar. [C<sub>6</sub>mim][NTf<sub>2</sub>]: Temperatures of 273.0 K, 303.0 K, 343.0 K, 383.0 K, 473.0 K at a pressure of 1 bar.
- [23] Each MD simulation consists of 173 ion pairs in the *NPT* ensemble using a Nosé-Hoover thermostat [36, 37] and the Rahman-Parrinello barostat [38, 39] with coupling times  $\tau_T = 0.5 \text{ps}$  and  $\tau_p = 2.0 \text{ps}$ . The electrostatic interactions are treated by Ewald summation [40] with a cutoff of 0.9 nm and a mesh spacing of approximately 0.12 nm with 4th order interpolation. Lennard-Jones cutoff corrections for energy and pressure were considered. A 2 fs timestep was used. Distance constraints were solved by the SHAKE procedure [41]. Our IL topology- and configuration-files are available from the Gromacs web site ([www.gromacs.org](http://www.gromacs.org)).
- [24] E. Lindahl, B. Hess, and D. van der Spoel, *J. Mol. Model.* **7**, 306 (2001).
- [25] D. Paschek, *J. Chem. Phys.* **120**, 6674 (2004).
- [26] M. P. Allen and D. J. Tildesley, *Computer Simulation of Liquids* (Oxford Science Publications, Oxford, 1989).
- [27] E. Wilhelm, B. R., and R. J. Wilcox, *Chem. Rev.* **77**, 219 (1977).
- [28] K. A. T. Silverstein, A. D. J. Haymet, and K. A. Dill, *J. Am. Chem. Soc.* **122**, 8037 (2000).
- [29] A. Ben-Naim, *Hydrophobic Interactions* (Plenum Press, New York, 1980).
- [30] A. D. J. Haymet, K. A. T. Silverstein, and K. A. Dill, *Faraday Discuss.* **103**, 117 (1996).
- [31] K. Lum, D. Chandler, and J. D. Weeks, *J. Phys. Chem. B* **103**, 4570 (1999).
- [32] S. Rajamani, T. Truskett, and S. Garde, *Proc. Natl. Acad. Sci. USA* **102**, 9475 (2005).
- [33] H. S. Ashbaugh and L. R. Pratt, *Rev. Mod. Phys.* **78**, 159 (2006).
- [34] H. S. Ashbaugh and L. R. Pratt, *J. Phys. Chem. B* **111**, 9330 (2007).
- [35] S. Klemmt, S. Dreyer, M. Eckstein, and U. Kragl, *Ionic Liquids in Synthesis* (Wiley-VCH, Weinheim, 2008), vol. 2, chap. 8, pp. 641–658, 2nd ed.
- [36] S. Nosé, *Mol. Phys.* **52**, 255 (1984).
- [37] W. G. Hoover, *Phys. Rev. A* **31**, 1695 (1985).
- [38] M. Parrinello and A. Rahman, *J. Appl. Phys.* **52**, 7182 (1981).
- [39] S. Nosé and M. L. Klein, *Mol. Phys.* **50**, 1055 (1983).
- [40] U. Essmann, L. Perera, M. L. Berkowitz, T. A. Darden, H. Lee, and L. G. Pedersen, *J. Chem. Phys.* **103**, 8577 (1995).
- [41] J. P. Ryckaert, G. Ciccotti, and H. J. C. Berendsen, *J. Comp. Phys.* **23**, 327 (1977).